International Journal of Plasticity 27 (2011) 1239–1251

Contents lists available at ScienceDirect

International Journal of Plasticity

journal homepage: www.elsevier.com/locate/ijplas

Creep and recovery of polypropylene/carbon nanotube composites

Yu Jia [a,b], Ke Peng [a], Xing-long Gong [b], Zhong Zhang [a,c,*]

[a] National Center for Nanoscience and Technology, No. 11 Beiyitiao Zhongguancun, Beijing 100190, China
[b] Department of Modern Mechanics, University of Science and Technology of China, Hefei 230027, China
[c] Center for Nano and Micro Mechanics, Tsinghua University, Beijing 100084, China

ARTICLE INFO

Article history:
Received 21 September 2010
Received in final revised form 14 December 2010
Available online 17 February 2011

Keywords:
Creep and recovery
Constitutive behavior
Mechanical testing
Nanocomposite
Carbon nanotube

ABSTRACT

The creep and recovery of polypropylene/multi-walled carbon nanotube composites were studied. It was found for thermoplastics in general that the creep strain reduces with decreased temperature, and with enhanced content of carbon nanotubes. The incorporation of nanotubes improved the recovery property remarkably, especially at high temperature. The unrecovered creep strain of nanocomposites with content of 1 and 2.8 vol.% carbon nanotubes decreased by 53% and 73% compared to that of polymer matrix. To understand the mechanisms, the Burger's model and Weibull distribution function were employed since the variations in the simulating parameters illustrated the influence of nano-fillers on the creep and recovery performance of the bulk matrix. To further study the recovery properties, the particular contribution of each Burger's element to the total deformation was obtained and the recovery percentage was calculated. The time–temperature–superposition-principle was applied to predict the long-term creep behavior.

1. Introduction

Polymer nanocomposites have gained enormous interests in science and engineering during the past decades due to their unique properties. Nanoparticles which may be dispersed on nanoscale can influence material properties more efficiently compared to micro-particles with the same volume content. Mechanical, magnetic, and electrical properties (Alig et al., 2007; Bao et al., 2008; Kanagaraj et al., 2007; Song et al., 2006; Zhang et al., 2010) of polymer nanocomposites have been extensively studied nowadays. For applications, many other performances, such as flame retardancy and gas permeability, are important issues.

Creep, as a time and temperature dependent phenomenon, is of importance for material applications requiring long-term durability and reliability (Aifantis, 1987; Krempl and Khan, 2003). Some studies on the creep performance of various materials were carried out, and the related modelings were developed accordingly (Barai and Weng, 2008). Creep deformation which causes by poor dimensional stability of thermoplastics, as an inherent defect, becomes a more serious problem (Morra et al., 2009). The effects of filling spherical nanoparticles and nanoclay into various thermoplastics associated with improved creep resistance have become one of the important issues in polymer nanocomposites. However, both positive and negative influences of fillers on the creep resistance of polymers have been reported. Some researchers (Ganß et al., 2007; Pegoretti et al., 2004; Vlasveld et al., 2005) obtained that the creep compliance could be decreased in thermoplastics filled with nanotubes and layered silicates. It was found that (Yang et al., 2006a,b) a dramatic increase of the creep resistance by adding various kinds of nanofillers, i.e. spherical particles and nanoclay, under different stress levels. Starkova et al. (2008) reported

* Corresponding author. Address: National Center for Nanoscience and Technology, No. 11 Beiyitiao Zhongguancun, Beijing 100190, China. Tel./fax: +86 10 82545586.
E-mail address: zhong.zhang@nanoctr.cn (Z. Zhang).

0749-6419/$ - see front matter © 2011 Elsevier Ltd. All rights reserved.
doi:10.1016/j.ijplas.2011.02.004

Nomenclature

a_T	temperature shift factor
C_1, C_2	coefficients in Eq. (8)
E'	storage modulus
E''	loss modulus
E_K	modulus of the Kelvin spring in the Burger's model
E_M	modulus of the Maxwell spring in the Burger's model
ΔH_m	melt enthalpy
ΔH_m°	coefficient in Eq. (1)
I	current intensity
n	time exponent in Eq. (9)
S	cross-sectional area
t	time
t_0	coefficient in Eq. (4)
T	temperature
T_0	reference temperature
U	applied voltage
ΔX	coefficient in Eq. (1)
X_c	crystallinity
X_R	percentage of recovery
X_ε	strain percentage of each element of Burger's model
β_r	shape parameter in Eq. (4)
ε_B	strain of the Burger's model
$\varepsilon_{element}$	strain of each element of Burger's model
ε_F	strain of the Findley power law
ε_{F0}	instantaneous initial strain of Findley power law
ε_{F1}	time-dependent creep strain
ε_{KV}	delayed elastic strain
ε_{MAX}	maximum creep strain
ε_{rvis}	time-dependent recovery strain
ε_{SM}	immediate elastic strain
ε_∞	permanent creep strain
η_K	viscosity of Kelvin dashpot in the Burger's model
η_M	viscosity of Maxwell dashpot in the Burger's model
η_r	characteristic life parameter in Eq. (4)
ρ_v	electrical resistivity
σ_0	stress
τ	retardation time

that the long-term tensile creep of polyamide 66 and its nanocomposites filled with only 1 vol.% TiO_2 nanoparticles, and a considerable enhancement in the creep resistance of the nanocomposites comparing the stress dependences of the viscoelastic strain components after different periods of creep. More recently, Siengchin and Karger Kocsis made a series of work (Siengchin, 2009; Siengchin and Karger-Kocsis, 2006, 2009) to prove that the creep resistance of thermoplastics can be effectively improved by adding nanoparticles such as nanoclay. In contrast, Shen et al. (2004) reported that the creep behavior of the nanocomposites showed an unexpected increasing trend as the clay loading increases (up to 5 wt.%). Additionally, these are only preliminary data and the role of nanoparticles on creep behavior is scantily reported. Some mechanisms have been provided (Yang et al., 2007) to explain the beneficial effects on the creep properties of polymers by incorporation of nanoparticles and they showed that the nanoparticles may inhibit slippage and reorientation of polymer chain, and thus improved long-term characteristics of thermoplastic polymers. Moreover, creep recovery is particularly significant in engineering applications. If the recovery ratio is too low, or the unrecovered strain is large after removing the applied stress, the material would suffer unpredictable damage. There were few literatures concerning specific recovery behavior of polymer nanocomposites. Muenstedt et al. (2008) found the recoverable shear creep compliance became smaller with decreasing nanoclay content. On the basis of the above findings, it seems that the study of nanocomposites on creep and recovery properties is still in its infancy, and current study on creep performance are mainly focused on layered silicate filled thermoplastic polymers. Accordingly, a major problem is the absence of systematic experimental research and the mechanism investigation of combining analysis and numerical simulations.

Carbon nanotubes (CNTs) have intrigued tremendous interests in scientific research owing to their outstanding structure and physical properties since the discovery (Iijima, 1991). Some modeling simulations were developed. For instance, Wu et al., 2008, 2009) have compared the atomistic-based shell theory with the atomistic simulation, and found that the numerical results of the former for the representative loadings under tension, torsion and bending agrees well with latter for CNTs.

Due to their combination of excellent mechanical characteristics, extremely large interfacial contact area, high aspect ratio, and low mass density, CNT are considered as the ideal reinforcement fillers for the composite materials (Eitan, 2005; Esawi and Farag, 2007; Lee et al., 2008; Pantano et al., 2008). The aim of the present work was to investigate that the incorporation of nanotubes improve the creep and recovery properties of PP under the conditions of different temperatures, especially the recovery property at a higher temperature. The modeling of creep and recovery properties of PP and its nanocomposites is satisfactorily conducted by using Burger's model and Weibull distribution function. Furthermore, in order to predict the long-term behavior based on experimental data, the time temperature superposition principle (TTSP) is employed and the predicting results confirm the enhanced creep resistance of nanotubes even at extended long time scale.

2. Experimental

2.1. Materials and preparation of nanocomposites

A commercial grade of PP (K1008, Sinopec) was considered as matrix material. Multiwalled carbon nanotubes (MWCNTs) were supplied by Chengdu Institute of Organic Chemistry, China, which were used as fillers. According to the supplier, the nanotubes have diameters of approximately 50 nm, lengths about 20 μm, and a carbon purity of 95% in weight.

In this work a two-step melt mixing strategy was used to improve the dispersion of fillers. In the first step a masterbatch 8.3 vol.% of MWCNT in PP was prepared in twin-screw extruder (Haake) operating at about 190 °C at 85 rpm. In the second step the PP/MWCNT masterbatch was diluted to attain right proportion of 0.3, 0.6, 1.7, 2.8, 4.4 vol.% (0.5%, 1%, 3%, 5%, 8% by weight). After cooling, the extruder blanks were cut as granules with length in a range of 3–5 mm for further injection molding.

The dispersion state of MWCNT was studied by scanning electron microscopy (SEM, HITAHI S-4800). Here, the cryo-fractured surfaces of the tensile loaded specimens were subjected to SEM inspection. The surfaces were gold coated prior to SEM performed at 6 kV acceleration voltage. Differential scanning calorimetry (DSC) traces were obtained using a differential scanning calorimeter (Diamond DSC, Perkin Elmer, USA) in the temperature range from −20 °C to 200 °C at a heating rate and cooling rate of 10 °C/min. The crystallinity (X_c) of PP was calculated from the following equation:

$$X_c = \frac{\Delta H_m}{(F \times \Delta H_m^\circ)} \times 100\% \tag{1}$$

where ΔH_m is the melt enthalpy of the PP in the sample and ΔH_m° is the theoretical enthalpy of PP for X_c = 100% (206 J/g), as reported in the literature (Van Krevelen, 1990). F is the volume fraction of matrix in the nanocomposites system.

2.2. Thermal analysis of composites

Thermo gravimetric analyses were done using TGA (Diamond, Perkin Elmer, USA) and a heating rate of 10 °C/min in air atmosphere for both pure polymers and nanocomposites.

Dynamic mechanical analysis (DMA) was made in tensile mode at 1 Hz frequency using a DMA Q800 apparatus (TA Instruments, USA). The specimens for DMA tests were molded with a compression machine at 210 °C and 20 MPa and the specimens' dimensions were 13 mm × 4.3 mm × 0.4 mm (length × width × thickness). The storage modulus (E') and loss modulus (E'') were determined as a function of the temperature, and the heating rate was set for 3 °C/min.

2.3. Tensile tests

Tensile test of the specimens was carried out with an universal testing machine (CMT2000, SANS, China). The granulated materials were injection molded into standard dumbbell-shaped specimens (30 × 3.1 × 3.3 mm^3, length × width × thickness, according to the ASTM D638 standard) by an injection molding machine (HAAKE MiniJet) for tensile tests. Measurements of the modulus were performed at room temperature with an electrical extensometer: a gauge length of 10 mm. The data of tensile strength and elongation at break was evaluated without an extensometer. The tests were carried out at a cross head speed of 2 mm/min. At least four specimens of each composition were tested, and the average values were reported.

2.4. Creep and creep–recovery measurements

Creep and creep–recovery tests were conducted in tensile mode under different temperatures using DMA. The specimens for creep and recovery tests were the same size as that of DMA tests. For each run, a new sample was used. The creep and recoverable strain were determined as a function of the time (t_{creep} = 30 min and $t_{recovery}$ = 120 min). Prior to the creep tests the stress level was derived from the stress–strain diagrams of the tensile tests and was fixed at 5 MPa (0.9% strain), to ensure the creep measurements remained in linear viscoelastic deformation regime.

The TTSP was adopted for short-term creep tests performed at various temperatures for PP and nanocomposites. The temperature range was 10–90 °C, in 5 °C steps, and the isothermal tests were run on the same specimen in the temperature range.

The 5 MPa creep stress was applied for 10 min at each temperature. Before each test prior to the measurement, the specimen was equilibrated for 5 min at each temperature, in order to evenly adjust for the correct temperature of the sample.

3. Results and discussion

3.1. Morphology of the nanocomposites

The SEM micrographs of the composites with 0.3, 0.6, 2.8 and 4.4 vol.% of MWCNTs are shown in Fig. 1. In order to characterize the state of distribution, a low magnification was selected. The nanotubes were fairly well dispersed in the nanocomposites with lower content of MWCNTs (Fig. 1a–c). The image of the composites with 2.8 vol.% of MWCNTs at high magnification reveals that the adhesion at interfaces between nanotubes and matrix is quite good (Fig. 1e). However, it is still difficult to completely disperse the MWCNTs in the PP matrix when the filler content increases to 4.4 vol.%. Some small nanotube aggregates can be observed in Fig. 1d and more details of the aggregates are shown in Fig. 1f. It can exhibit that the powdery nanotube aggregates (prior to mixing) were infiltrated by the neat matrix during the melt-mixing process.

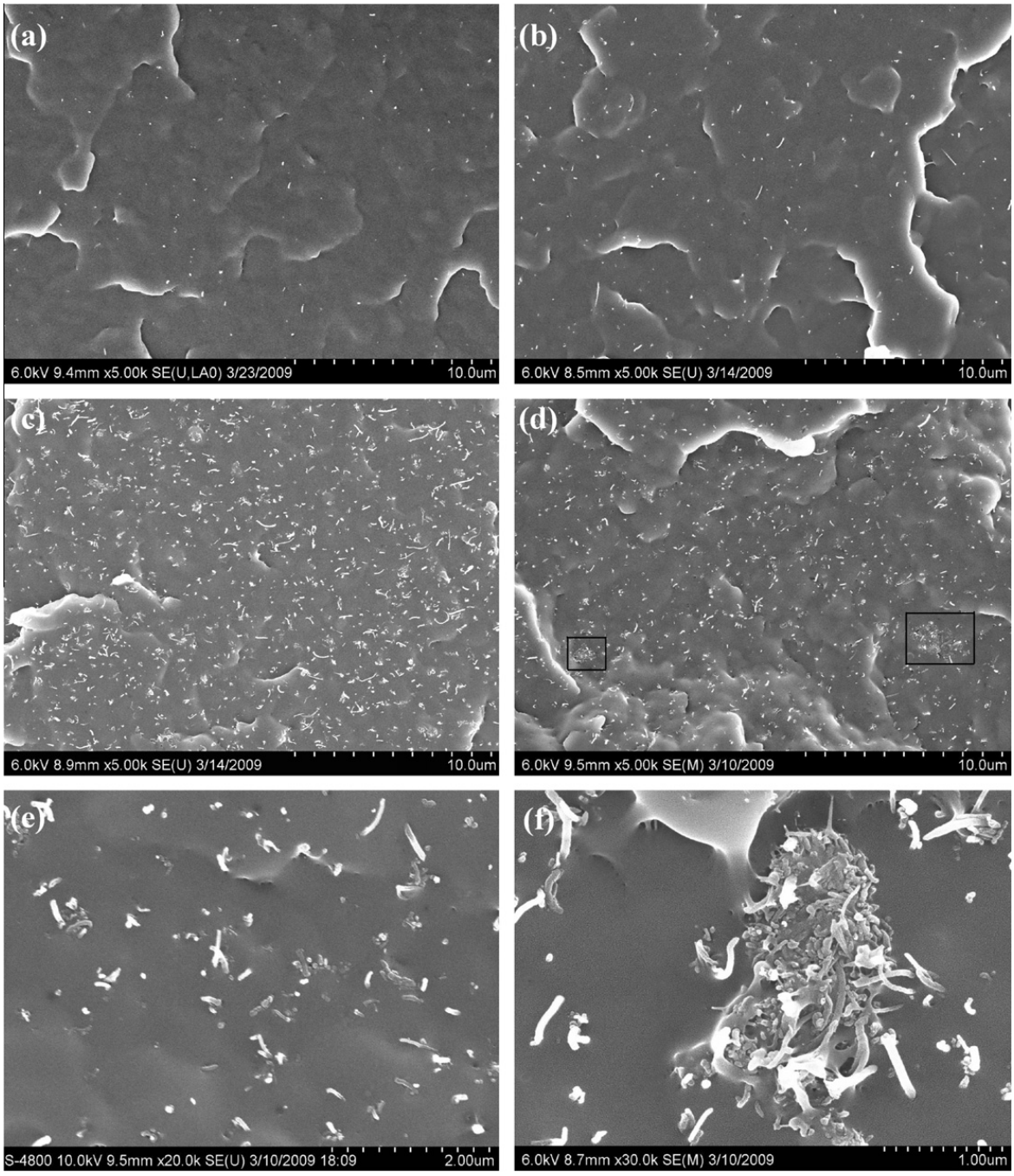

Fig. 1. SEM micrographs of PP/MWCNT nanocomposites with filler content of (a) 0.3 vol.%; (b) 0.6 vol.%; (c) and (e) 2.8 vol.%; (d) and (f) 4.4 vol.%.

The DSC results are shown in Fig. 2. By calculation, the crystallinity of nanocomposites with 0, 0.3, 0.6, 2.8 and 4.4 vol.% of MWCNTs are 56.3%, 56.4%, 58.5%, 57.7% and 59.6%, respectively. The overall crystallinity is increasing by the incorporation of MWCNT in PP. Some research groups reported that CNTs might act as nucleating agent during isothermal process which possibly brings to increase the degree of crystallinity (Yang et al., 2007). Fig. 2b shows an increase in crystallization temperature with increase in MWCNT content.

3.2. Thermomechanical properties

DMA spectra in form of as function storage modulus (E') and loss modulus (E'') of temperature are plotted and are demonstrated in Fig. 3a and b, respectively. One can recognize that the incorporation of nanotubes results in the increase of the storage modulus in the whole temperature range, compared to that of neat PP. This can well be explained by the reinforcing effect of the nanoparticles leading to increased stiffness. In comparison, the greater modulus enhancement occurs at high temperature than that at low temperature. The glass transition temperature, as determined from DMA (Fig. 3b), is observed to show unaffected by the adding of nanotubes.

Adding MWCNTs can increase the thermal stability of PP in accordance with our TGA observation (Fig. 3c). It can be seen that the resistance to thermooxidative degradation of PP/MWCNT composites become higher with the increase in concentration of carbon nanotubes. This fact can be observed, for example, the composite with only 0.6 vol.% of MWCNT content started to degrade markedly at higher temperature than pure PP. However, there is practically no difference between the TGA traces of the composites with 2.8 vol.% and 4.4 vol.% of MWCNT content.

3.3. Tensile properties

The tensile properties of the materials at room temperature have been determined. The Young's modulus, tensile strength and elongation at break are listed in Table 1 with relative deviation. In general, the Young's modulus and the tensile strength of the composites were slightly higher than that of matrix, showing the reinforcing effect of MWCNT. Among them, the Young's modulus of composites with content of 0.3 vol.% and 2.8 vol.% MWCNT increase by 15% and 32%, respectively, compared to that of neat PP. The total elongation of nanocomposites was decreased greatly while shows brittleness to some degrees.

3.4. Creep and recovery behavior

Fig. 4 displays the traces of the creep and recovered strains as a function of time for the composites with 0, 0.3, 0.6, 2.8 vol.% of MWCNT content, respectively, in three different temperature conditions. In the experimental test 5 MPa was carefully selected as the applied stress within the elastic range. In these curves, the creep stages (instantaneous deformation, primary and secondary creeps) can be clearly observed. On the other hand, there was no evidence of tertiary creep, i.e. creep rupture, which would require longer time and larger stress. As it is expected, creep strain increased with temperature, at the same time similar behavior was displayed by the nanocomposites. It is visibly apparent that with the raising of the temperature from −50 °C to 80 °C the creep strain can increase by 900% approximately, at $t = 1800$ s. Thus, the value of the creep strain toward the temperature change is very sensitive. Furthermore, the results shown in Fig. 4 can also indicate that creep strains of nanocomposites were lower than that of the neat matrix at all test temperatures and this implies that

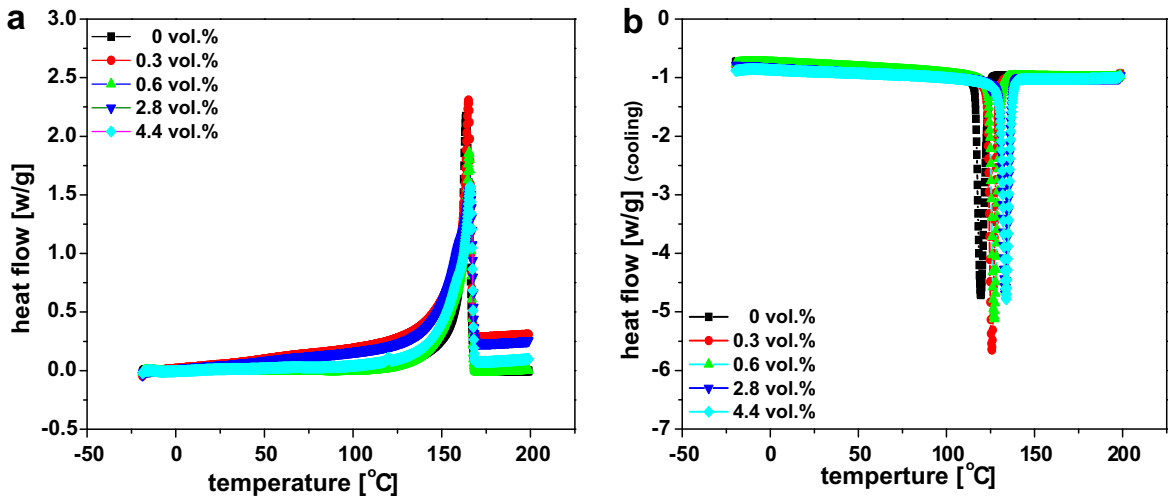

Fig. 2. DSC thermograms showing (a) heating and (b) cooling curves of PP/MWCNT nanocomposites.

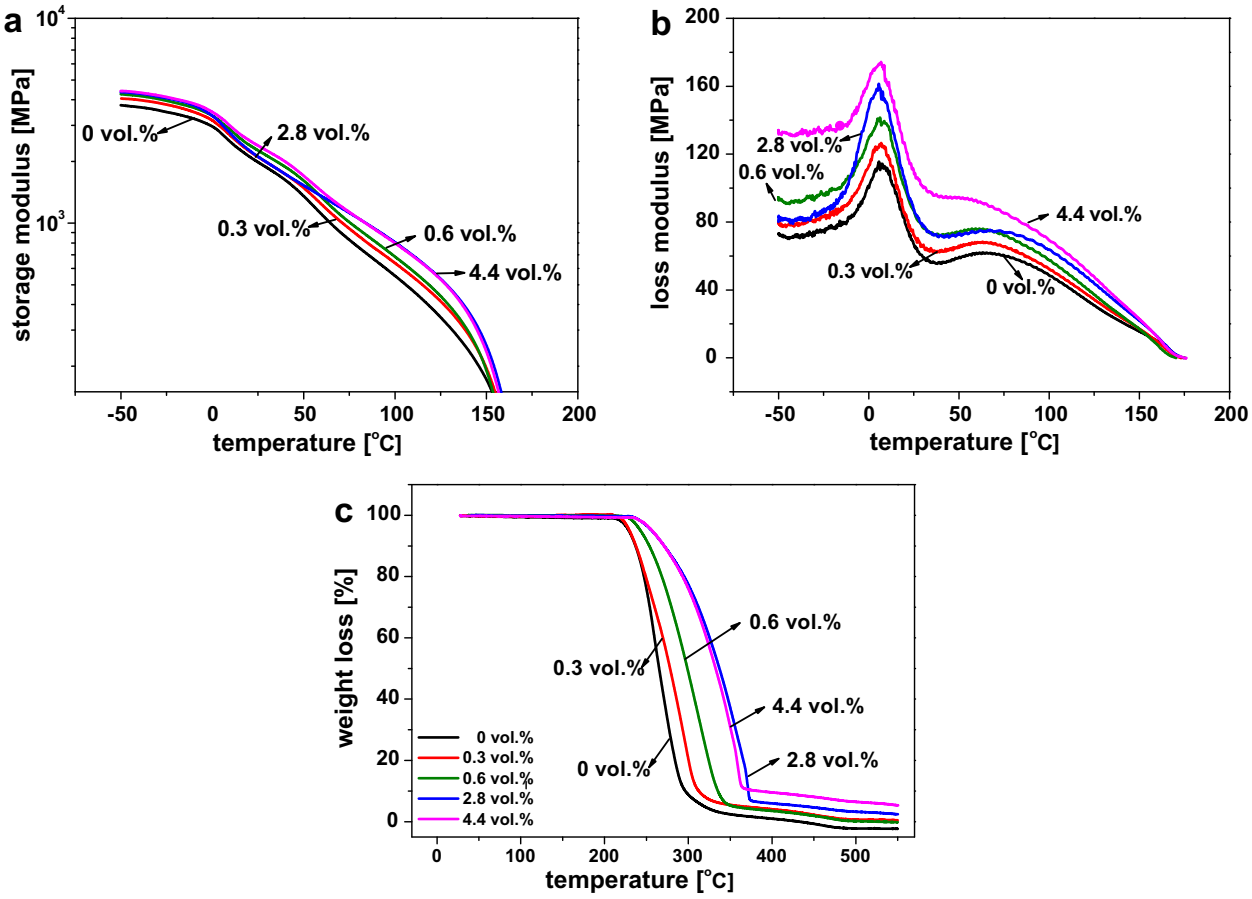

Fig. 3. (a) Storage modulus, (b) loss modulus and (c) weight loss versus temperature of PP/MWCNT nanocomposites.

Table 1
Tensile mechanical characteristics of the PP and PP/MWCNT nanocomposites with deferent MWCNT contents.

MWCNTs content (vol.%)	Young's modulus (GPa)	Tensile strength (MPa)	Elongation at break (%)
0	1.83 ± 0.11	36.1 ± 0.3	711.4 ± 87.6
0.3	2.10 ± 0.11	38.6 ± 0.6	472.2 ± 27.2
0.6	2.12 ± 0.03	39.0 ± 0.4	439.2 ± 15.6
2.8	2.33 ± 0.14	40.0 ± 3.2	53.2 ± 5.8
4.5	2.42 ± 0.13	40.4 ± 0.3	68.2 ± 19.8

the creep behavior is improved by the presence of nanotubes. For example, the strain values at 80 °C were reduced by 11%, 21% and 36% compared to polypropylene when the contents of MWCNT were 0.3 vol.%, 0.6 vol.% and 2.8 vol.%, respectively. In addition, it is also observed that the creep strain rate increased with temperature and MWCNT content as shown in Fig. 5. One can recognize that the creep strain rate decreased remarkably with the incorporation of MWCNT, and for example, at 80 °C the creep rate of composites containing 0.3, 0.6 and 2.8 vol.% MWCNT decreased by 40%, 58%, 72%, respectively.

The course of the recovered strain as a function of time is also presented in Fig. 4. While the greater elasticity at higher temperature is recovered, a larger permanent deformation of the viscoelastic and viscous response are observed. The unrecovered strain of pure PP increased by 56 and 10 times at the temperatures of 25 °C and 80 °C compared with −50 °C, respectively. Moreover, the curves also indicate that incorporation of nanotubes improves the elastic recovery and decreases the recovered strain remarkably. It is found that the recoverable strain of the nanocomposites decreases with the content of MWCNT over the whole relaxation time range. To be emphasized is that at higher temperature the reduction of recovered strain has become increasingly. These findings suggest that creep and recovery behaviors are suitable indicators for the impact of the fillers and temperature.

The Burger's (or four parameters) model, a combination of Maxwell and Kelvin–Voigt elements, is one of the most used models to give the relationship between the morphology of the composites and their creep behavior (Ward, 1983; Findley et al., 1989). For the most general case of a linear viscoelastic solid, the total strain is the sum of three essentially separate parts: ε_{SM} the immediate elastic deformation, ε_{KV} the delayed elastic deformation and ε_{∞} the Newtonian flow, which is identical with the deformation of a viscous liquid obeying Newton's law of viscosity. The total strain as a function of time corresponds to the following equation:

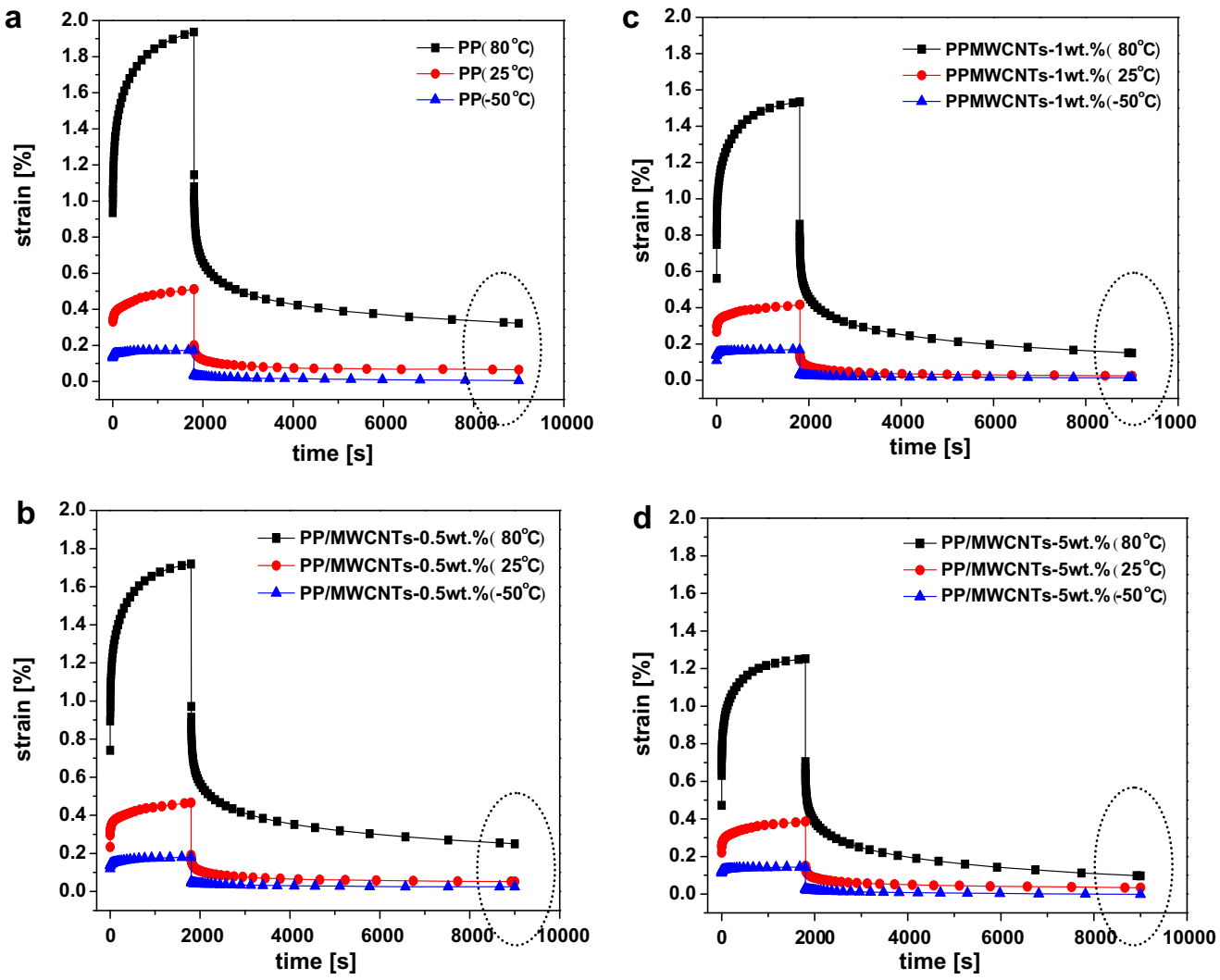

Fig. 4. Temperature dependent creep strain: (a) neat PP; (b) PP + 0.3 vol.%; (c) PP + 0.6 vol.%; and (d) PP + 2.8 vol.% MWCNT.

$$\varepsilon_B = \varepsilon_{SM} + \varepsilon_{KV} + \varepsilon_\infty \tag{2}$$

$$\varepsilon_B = \frac{\sigma_0}{E_M} + \frac{\sigma_0}{E_K}(1 - e^{-t/\tau}) + \frac{\sigma_0}{\eta_M} t \tag{3}$$

Here, t denotes time after loading, E_M and η_M are the modulus and viscosity of the Maxwell spring and dashpot, respectively; E_K and η_K are the modulus and viscosity of the Kelvin spring and dashpot, respectively; $\tau = \eta_K/E_K$ is the retardation time taken to produce 63.2% or $(1 - e^{-1})$ of the total deformation in the Kelvin unit. The experimental curves of creep phase at higher temperature ($T = 80$ °C) were fitted by means of Burger's model as shown in Fig. 6a. The non-linear curve fit function of the OriginPro 7.5 software was used and four parameters (E_M, E_K, η_K and η_M) were defined. As shown in Fig. 6a the modeling curves show a satisfactory agreement with the experimental data. The values of four parameters for the matrix and nanocomposites are summarized in Table 2, and it shows that all of these parameters display an increasing trend with the content of nanotubes. The parameter E_M associated to the Maxwell spring establishes instantaneous creep strain that would be recovered after stress elimination. The result shows that the nanotubes are able to improve the elasticity of the pure PP, which is consistent with the results of tensile tests. The retardant elasticity E_K is related to the stiffness of amorphous polymer chains in short term, and it also increases with the content of MWCNT, which reflects the reinforcement of nanotubes on the Kelvin–Voigt unit. η_K indicates the viscosity of the Kelvin–Voigt unit, and the ratio of η_K to E_K is the relaxation time τ. Both parameters, τ and η_K seems to increase with MWCNT incorporation. A more important parameter η_M is also listed in Table 2, which represents the irrecoverable creep strain and is much higher than η_K, and is sensitive to the content of MWCNT. As can be seen from the fitting results, the viscosity η_M increases with MWCNT content and lower flow was occurred at the dashpot and the permanent deformation decreased. In order to further illustrate the character of nanotubes in deceasing the viscous flow deformation (or irrecoverable creep deformation) remarkably at higher temperature, the Weibull distribution equation was applied as following to simulate the recovery part of the experimental data at 80 °C.

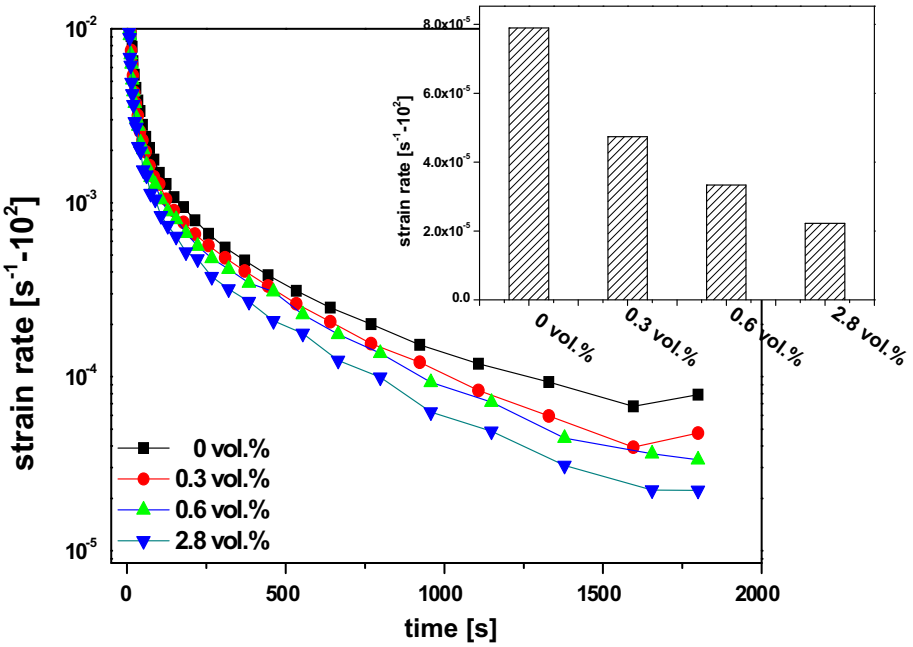

Fig. 5. Creep rates of PP and PP/MWCNT nanocomposites with different filler content as a function of time at 80 °C.

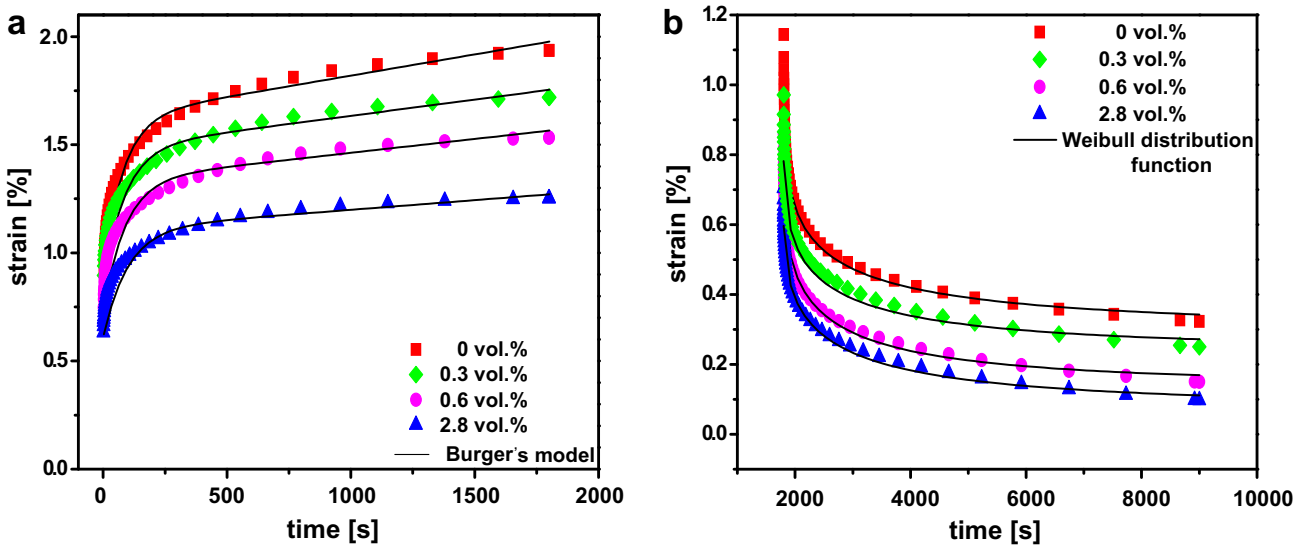

Fig. 6. Modeling results of creep and recovery curves for short creep tests obtained at 80 °C: (a) fitting creep phase by Burger's model and (b) fitting recovery phase by Weibull distribution function.

Table 2
The simulated parameters of the Burger's model and the Weibull distribution function with different MWCNT contents for short creep tests at 80 °C.

MWCNT content (vol.%)	E_M (MPa)	E_K (MPa)	η_K (MPa s)	η_M (s)	τ (s)	ε_r (%)	η_r (s)	β_r	ε_f (%)
0	5.5	7.0	565	25,500	80.7	0.71	10.87	0.39	0.30
0.3	5.9	7.9	691	33,304	87.9	0.59	13.89	0.42	0.24
0.6	6.9	8.2	730	39,000	89	0.64	14.08	0.43	0.14
2.8	8.2	10	1000	56,000	100	0.54	20.05	0.46	0.08

The Weibull distribution function (Fancey, 2005) has been successfully fitted to the recovery data of semi-crystalline polymers from a wide range of sources. On removing the load, there may be some instantaneous (elastic) strain recovery, which is then followed by time-dependent recovery strain:

$$\varepsilon_{rvis}(t) = \varepsilon_{KV}\left[\exp\left(-\left(\frac{t-t_0}{\eta_r}\right)^{\beta_r}\right)\right] + \varepsilon_{\infty} \tag{4}$$

where, the ε_{KV} function, for viscoelastic strain recovery, is determined by the characteristic life (η_r) and shape (β_r) parameters over recovery time t, and t_0 is the time of stress removed. ε_{∞} is the permanent strain from viscous flow effects. Additionally, the value of ε_{KV} and ε_{∞} can be received through the simulation of Weibull equation, and ε_{MAX} is the maximum deformation corresponding to the strain value for the longest time (t_0 = 1800 s) during the creep test. The fits of the experimental curves of the recovery strain as a function of time are shown in Fig. 6b. On repeating the fits with these parameters, we obtained the strain values of the Maxwell dashpot and of the Kelvin–Voigt elements, respectively, ε_{KV} and ε_{∞}. The results obtained, together with the parameters η_r and β_r, are shown in Table 2. It is apparent that the parameters ε_{KV} and ε_{∞} decreased with MWCNT content which indicates an enhanced recovery performance. On the other hand, both the characteristic life factor η_r and shape factor β_r show an increasing trend with the concentration of nanotubes, and the latter parameter may reflect the change of the creep rate of nanocomposites. Combining the analysis of the two models, it can indicates that, adding carbon nanotubes may lead to an increase in viscosity, thus MWCNT inhibit the slippage of molecular chains of polymer. That is to say, the increasing of viscosity (which reflects by the parameter η_M) results in the sharply decreasing of the permanent strain (which reflects by the parameter ε_{∞}), accordingly the recovery property of nanocomposites were improved remarkably.

The recovery of the system after stress elimination presents characteristics what are different to those of creep. All recovery tests comprise three essentially separate parts (in Fig. 7) once the source of stress is removed: the first recovery, ε_{SM}, is instantaneous and corresponds to the spring of the Maxwell element. Second recovery, ε_{KV}, is slower of a decreasing exponential type, and tending towards a asymptote for $t \to \infty$. ε_{KV} is due to the Kelvin–Voigt element. Lastly is the Newtonian flow, ε_{∞}, which is identical with the deformation of a viscous liquid obeying Newton's law of viscosity, due to sliding of the Maxwell dashpot, which determines permanent deformation due to the irreversibility of the mentioned slide. As mentioned above, the value of ε_{KV} and ε_{∞} can be received through the simulation of Weibull equation, so the deformation suffered by the Maxwell spring, or instantaneous strain ε_{SM}, can be obtained by using Eq. (5):

$$\varepsilon_{SM} = \varepsilon_{MAX} - (\varepsilon_{KV} + \varepsilon_{\infty}) \tag{5}$$

We use Eq. (5) to calculate the strain, ε_{SM}, corresponding to the Maxwell spring, and list the strain of each element of the Burger's model, ε_{SM}, ε_{KV}, ε_{∞}, ε_{MAX}, in Table 3. Consequently, the strains of each element of the Burger's model can be acquired. On the other hand, full mechanical characterization of a system need to be established by calculating the contribution of each of the parts of the model and determining the maximum deformation that the system is subjected. The strain percentage of each element of the Burger's model can be calculated by the following equation:

$$X_{\varepsilon} = \left[\frac{\varepsilon_{element}}{\varepsilon_{MAX}}\right] \times 100\% \tag{6}$$

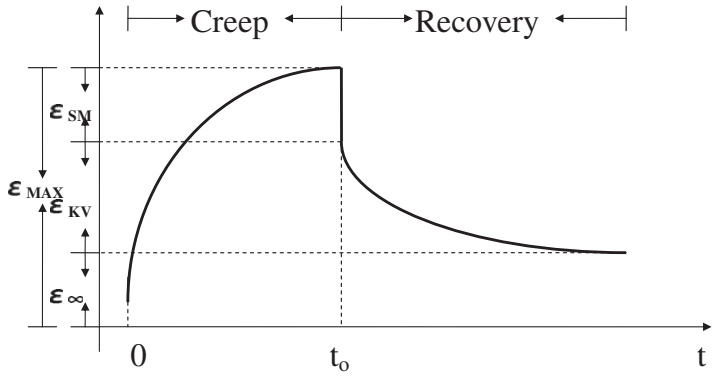

Fig. 7. Strain versus time for the Burger's model in a creep and recovery test.

Table 3
The calculated value and percentage of each element of Burger's model and the recovery ratio with the MWCNT content.

MWCNT content (vol.%)	Value			Percentage of Burger's model			
	ε_{SM} (%)	ε_{KV} (%)	ε_{∞} (%)	$X\varepsilon_{SM}$ (%)	$X\varepsilon_{K}$ (%)	$X\varepsilon_{\infty}$ (%)	$X_{recovery}$
0	0.93	0.71	0.3	47.90	36.60	15.50	84.50
0.3	0.89	0.59	0.24	51.70	34.30	14.00	86.00
0.6	0.75	0.64	0.14	49.00	14.00	9.20	90.80
2.8	0.63	0.54	0.08	50.40	86.00	6.40	93.60

As all the values of each element have obtained, we can use Eq. (6) to calculate the contribution to the total deformation of the system of the two components of the Maxwell element and the Kelvin–Voigt element as shown in Table 3. The results as mentioned above are in agreement with the reinforcement of the nanotubes. As can be seen, with the increasing MWCNT content, the strain of each element become decreasing. The contribution of the Maxwell element (the sum of ε_{SM} and ε_{∞}) to total deformation is much higher than the Kelvin–Voigt element, and adding nanotubes in the matrix can reduce the disparity between the two elements. Remarkably, the permanent creep strain (ε_{∞}) of the composites is quite smaller than neat PP, and this result means that carbon nanotubes can largely reduce the viscous flow deformation of materials. Among them the permanent creep strains of composites with content of 0.3 vol.% and 2.8 vol.% MWCNT increase by 53% and 73%, respectively, compared to that of neat PP.

On the basis of the available data, it is also not difficult to determine the final percentage recovery of each of the systems. By means of ε_{∞} which obtains by the simulation of the Weibull distribution function, the final percentage recovery of a system is defined as following:

$$X_R = \left[\frac{\varepsilon_{\mathrm{MAX}} - \varepsilon_{\infty}}{\varepsilon_{MAX}}\right] \times 100\% \tag{7}$$

The values obtained by Eq. (7), are reported in Table 3. It is very clearly that the percentage recovery of the nanocomposites is much higher than the matrix due to reinforcement of the nanotubes.

Based on the aforementioned experimental results and model simulation, the mechanisms from the molecular perspective are considered that could contribute to the observed enhancement of creep and recovery properties. The carbon nanotubes were dispersed into the amorphous region of PP and had a good interface with the polymer matrix. When the external mechanical loading was applied to the nanocomposites, the location of nanotubes can increasing immobility of amorphous region acting as blocking sites. Note that The MWCNT incorporation can impact on several aspects of immobility of molecules, such as the stretching of chain segment and slippage between molecular chain, wherefore the creep strain is decreased and the creep resistance of PP/MWCNTs are enhanced. On the other hand, in the Burger's model three parts of strain of the nanocomposites, ε_{SM}, ε_{KV}, ε_{∞}, were decreased by adding nanotubes, and especially the permanent creep strain (ε_{∞}). As mentioned above from the analysis about Weibull distribution function, ε_{∞} is an important parameter which directly related to the recovery property of materials. Note that the ε_{∞} is due to the relative slippage between molecules chain. Accordingly the improvement of recovery property is due to the fact that, MWCNT inhibit the slippage of molecular chains of polymer, thus make the viscosity increased, the permanent strain (ε_{∞}) decreased and recovery strain increased.

3.5. Prediction by TTSP

The TTSP has been widely used to obtain the master curves for a given property as a function of time or time-related quantities like creep (Ward, 1983). In the current investigation, creep experiments of PP and nanocomposites were performed at different temperature levels and the relevant creep curves obtained. All the individual creep curves corresponding to different temperature levels were shifted along the logarithmic time axis to superpose to a master curve. The shifting procedure of this curve obeys the Williams–Landel–Ferry (WLF) equation. The WLF equation given by:

$$\log a_T) = \frac{-C_1(-T_0)}{C_2 + (T - T_0)} \tag{8}$$

The master curves which are presented as creep compliance are shown in Fig. 8. It indicates the prediction of the long-term property of nanocomposites, and extends up to more than 10^{11} s in time scale. The insertion graph of Fig. 8 demonstrates that the WLF equation adequately describes the temperature dependence of the shift factors of neat PP and nanocomposites studied. The shift factor showed a good linear dependence on the temperature. The master curves show that the creep compliance of composites with increasing MWCNT content was obviously lower than that of PP, which indicates the reinforcing effectiveness of carbon nanotubes. However, it is interesting to note that, above 10^6 s, the increment of compliance with time show a tendency of faster increase and the matrix is easy to be influenced by nanoparticles. These findings show that under the small stress the materials entered into a viscoelastic state over an extremely long period of time, and in viscoelastic state the carbon nanotubes play a better role in the reinforcement of materials. Strikingly, from the master curves, the nanocomposites with 0.3 vol.% of MWCNT has shown a tendency of faster decrease in creep compliance, which indicates that a quite low content of carbon nanotubes can enhance creep resistance of materials to a large extent. However, the creep compliances of nanocomposites present a trend with the increasing concentration of MWCNT except the composites with 4.4 vol.% of MWCNT. The phenomena may relate to two reasons. Firstly, with the higher content of nanotubes, it is difficult to disperse the nanoparticles uniformly in the matrix, and so there are more aggregation existing in the nanocomposites with higher content of MWCNT. The aggregation may lead to the reduction of creep resistance accordingly. Secondly, when the content of nanotubes reach to a threshold value, enhancement effect with nanotubes may be limited, for instance, the master curves of nanocomposites with 2.8 vol.% and 4.4 vol.% of MWCNT have almost the same shape. A similar observation can also be obtained by TGA, DMA and tension tests (mentioned above). But at the moment we have not yet got the precise value as the threshold, which needs further study.

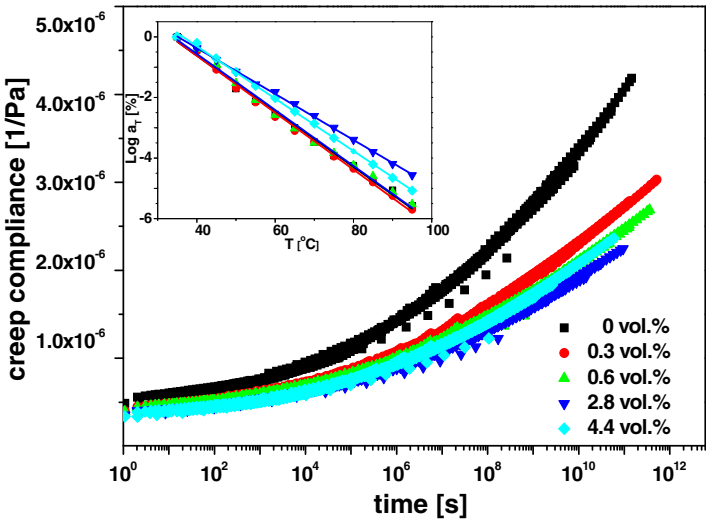

Fig. 8. The master curves showing creep compliances as a function of time. The insertion graph shows the shift factor, log a_T, as a function of temperature.

The viscoelastic behavior of thermoplastic composites could also be modeled by using a constitutive model based on an empirical power law equation known as Findley power law (Findley et al., 1989):

$$\varepsilon_F = \varepsilon_{F0} + \varepsilon_{F1} t^n \tag{9}$$

In Eq. (9), ε_F is the total creep strain at time t, ε_{F0} is the instantaneous initial strain, ε_{F1} is the time-dependent creep strain and n is the time exponent which is independent of stress. Attempt was also made to check whether the Findley power law and the four parameters model predict the creep of our systems properly. Note that the parameters of burger's model display the same trend here as the ones described in the previous subsection, so there is no repeated analysis here.

By comparison of the predicting ability of the Burger's model and Findley power law for PP and the nanocomposites as shown in Fig. 9, it could obviously be seen over that Findley power law is a satisfactory means to predict the long-term creep

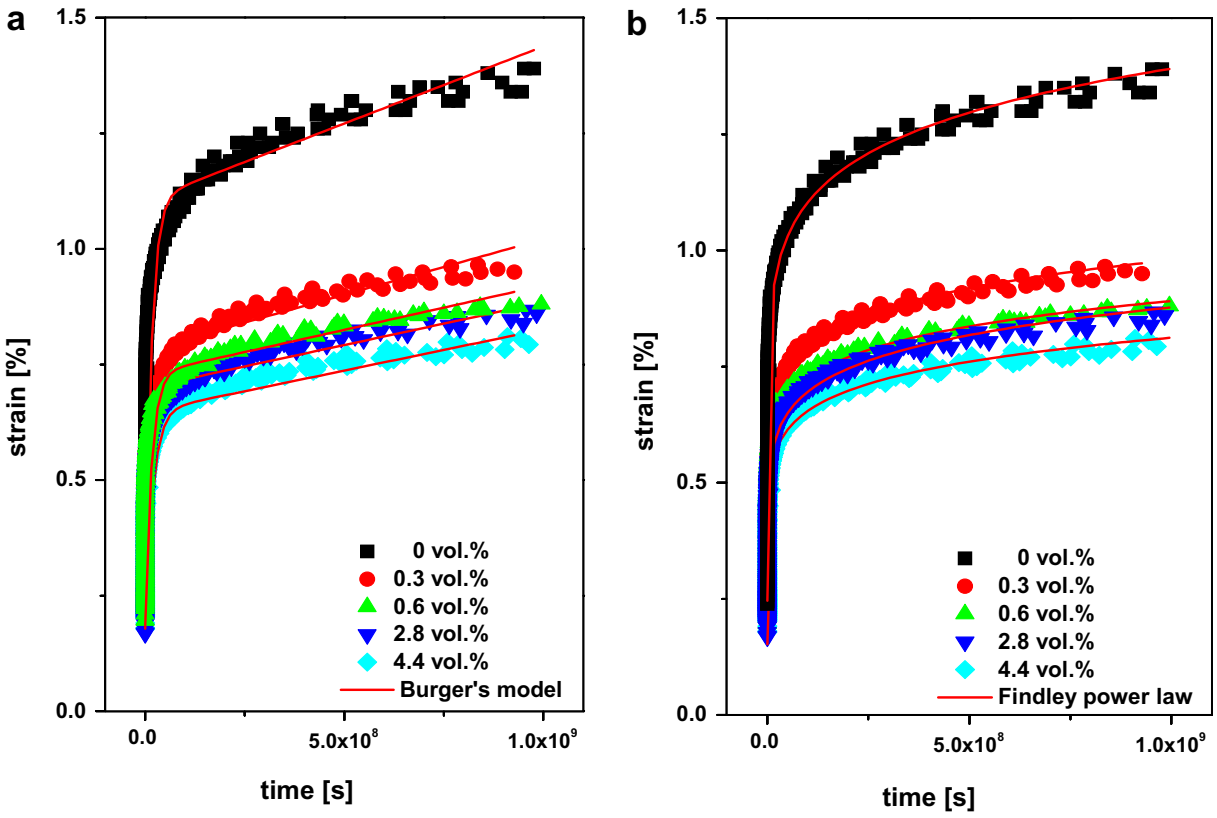

Fig. 9. Modeling results of creep curves for long term prediction by (a) Burger's model and (b) Findley power law.

Table 4
The simulated parameters of the Burger's model and the Findley power law with different MWCNT contents for long term prediction.

MWCNT content (vol.%)	E_M (MPa)	E_K (MPa)	η_K (MPa s)	η_M (s)	τ (s)	ε_{F0} (%)	ε_{F1} ($10^2 \cdot (s^n)^{-1}$)	n
0	22.1	5.7	9.00E+07	1.50E+10	1.49E+07	0.119	0.126	0.112
0.3	26.0	8.5	1.00E+08	2.10E+10	1.53E+07	0.094	0.106	0.102
0.6	27.0	9.2	1.50E+08	2.60E+10	1.63E+07	0.089	0.097	0.102
2.8	28.1	9.6	1.70E+08	2.70E+10	1.77E+07	0.081	0.082	0.106
4.5	29.9	10.4	2.00E+08	2.80E+10	1.92E+07	0.071	0.081	0.111

performance, and the prediction of the Burgers model, however, shows some deviation from the experimental data. The values of related parameters for the matrix and nanocomposites are summarized in Table 4. It is apparent that the parameters of Findley power law, the instantaneous initial creep strain ε_{F0} and the time-dependent creep strain ε_{F1}, decreased with the content of nanotubes which indicates an enhanced creep performance. In addition, n of each specimen was not affected by MWCNT incorporation.

4. Conclusions

This paper studied the creep and recovery behavior of PP/MWCNT nanocomposites compounded using a twin-screw extruder. The creep strain was increased with temperature and decreased with the content of carbon nanotubes indicates an enhanced performance at short time scales. It also indicated that the incorporation of nanotubes decreased the recovered strain remarkably at higher temperatures. The modeling of creep and recovery properties of PP and its nanocomposites were satisfactorily conducted by using Burger's model and Weibull distribution function. The parameters also confirmed that the instantaneous and retardant modulus increased and the permanent viscosity, relaxation time and permanent creep strain decreased as a function of MWCNT content. Combining the analysis of the two models, it can indicate that the increasing of viscosity results in the decreasing of the permanent strain and it was probably because MWCNT inhibited the slippage of molecular chains of polymer. To further study the recovery properties, the particular contribution of each of the Burger's elements to the total deformation of the system were obtained and the recovery percentage of each system was quantitatively discussed.

The master curves which constructed by using the time temperature superposition principle indicated the prediction of the long-term property of nanocomposites, and extends up to more than 10^{11} s in time scale. The nanocomposites with 0.3 vol.% of MWCNT showed a tendency of faster decrease in creep compliance, which indicates that a quite low content of carbon nanotubes can enhance creep resistance of materials to a large extent. Both Findley power law and Burger's model were used to predict the long-term creep of the polymer nanocomposites.

Acknowledgements

This project was jointly supported by the National Key Basic Research Program of China (Grant No. 2007CB936803) and a key international collaboration project (Grant No. 2008DFA51220) of the Ministry of Science and Technology of China, a key item of the Knowledge Innovation Project of the Chinese Academy of Science (Grant No. KJCX2-YW-M01) and the National Nature Science Foundation of China (Grant No. 51073044).

References

Aifantis, E.C., 1987. The physics of plastic deformation. Int. J. Plasticity 3, 211–247.
Alig, I., Lellinger, D., Dudkin, S.M., Potschke, P., 2007. Conductivity spectroscopy on melt processed polypropylene-multiwalled carbon nanotube composites: recovery after shear and crystallization. Polymer 48, 1020–1029.
Bao, H.D., Guo, Z.X., Yu, J., 2008. Effect of electrically inert particulate filler on electrical resistivity of polymer/multi-walled carbon nanotube composites. Polymer 49, 3826–3831.
Barai, P., Weng, G.J., 2008. Mechanics of creep resistance in nanocrystalline solids. Acta Mech. 195, 327–348.
Eitan, A., 2005. Reinforcement mechanisms in MWCNT-filled polycarbonate. Compos. Sci. Technol. 66, 1162–1173.
Esawi, A.M.K., Farag, M.M., 2007. Carbon nanotube reinforced composites: potential and current challenges. Mater. Des. 28, 2394–2401.
Fancey, K.S., 2005. A mechanical model for creep, recovery and stress relaxation in polymeric materials. J. Mater. Sci. 40, 4827–4831.
Findley, W.N., Lai, J.S., Onaran, K., 1989. Creep and Relaxation of Nonlinear Viscoelastic Materials: With an Introduction to Linear Viscoelasticity. Dover Publications, Inc., New York.
Ganß, M., Satapathy, B.K., Thunga, M., Weidisch, R., Potschke, P., Janke, A., 2007. Temperature dependence of creep behavior of PP–MWNT nanocomposites. Macromol. Rapid Commun. 28, 1624–1633.
Iijima, S., 1991. Helical microtubules of graphitic carbon. Nature 354, 56–58.
Kanagaraj, S., Varanda, F.R., Zhil'tsova, T.V., Oliveira, M.S.A., Simoes, J.A.O., 2007. Mechanical properties of high density polyethylene/carbon nanotube composites. Compos. Sci. Technol. 67, 3071–3077.
Krempl, E., Khan, F., 2003. Rate (time)-dependent deformation behavior: an overview of some properties of metals and solid polymers. Int. J. Plasticity 19, 1069–1095.
Lee, G.W., Jagannathan, S., Chae, H.G., Minus, M.L., Kumar, S., 2008. Carbon nanotube dispersion and exfoliation in polypropylene and structure and properties of the resulting composites. Polymer 49, 1831–1840.
Morra, P.V., Morra, P.V., Radelaar, S., Yandouzi, M., Chen, J., Bottger, A.J., 2009. Precipitate coarsening-induced plasticity: low temperature creep behaviour of tempered SAE 52100. Int. J. Plasticity 25, 2331–2348.

Muenstedt, H., Katsikis, N., Kaschta, J., 2008. Rheological properties of poly(methyl methacrylate)/nanoclay composites as investigated by creep recovery in shear. Macromolecules 41, 9777–9783.
Pantano, A., Modica, G., Cappello, F., et al, 2008. Multiwalled carbon nanotube reinforced polymer composites. Mater. Sci. Eng. A – Struct. 486, 222–227.
Pegoretti, A., Kolarik, J., Peroni, C., Migliaresi, C., 2004. Recycled poly(ethylene terephthalate)/layered silicate nanocomposites: morphology and tensile mechanical properties. Polymer 45, 2751–2759.
Starkova, O., Zhang, Z., Zhang, H., 2008. Limits of the linear viscoelastic behaviour of polyamide 66 filled with TiO_2 nanoparticles: effect of strain rate, temperature, and moisture. Mater. Sci. Eng. A – Struct. 498, 242–247.
Siengchin, S., 2009. Long- and short-term creep of polyoxymethylene/polyurethane/alumina ternary composites by comparison. Mech. Compos. Mater. 45, 415–422.
Siengchin, S., Karger-Kocsis, J., 2006. Creep behavior of polystyrene/fluorohectorite micro- and nanocomposites. Macromol. Rapid. Commun. 27, 2992–3002.
Siengchin, S., Karger-Kocsis, J., 2009. Structure and creep response of toughened and nanoreinforced polyamides produced via the latex route: effect of nanofiller type. Compos. Sci. Technol. 69, 677–683.
Shen, L., Phang, I.Y., Chen, L., Liu, T.X., Zeng, K.Y., 2004. Nanoindentation and morphological studies on nylon 66 nanocomposites. I: Effect of clay loading. Polymer 45, 3341–3349.
Song, B., Chen, W.N., Liu, Z.S., Erhan, S., 2006. Compressive properties of epoxidized soybean oil/clay nanocomposites. Int. J. Plasticity 22, 1549–1568.
Van Krevelen, D.W., 1990. Properties of Polymers. Elsevier, Amsterdam.
Vlasveld, D.P.N., Bersee, H.E.N., Picken, S.J., 2005. Creep and physical aging behaviour of PA6 nanocomposites. Polymer 46, 12539–12545.
Ward, I.M., 1983. Mechanical Properties of Solid Polymers. John Wiley and Sons Ltd., Weinheim.
Wu, J., Hwang, K.C., Huang, Y., 2008. An atomistic-based finite-deformation shell theory for single-wall carbon nanotubes. J. Mech. Phys. Solids 56, 279–292.
Wu, J., Zhang, Z., Liu, B., Hwang, K.C., Huang, Y., 2009. Numerical analyses for the atomistic-based shell theory of carbon nanotubes. Int. J. Plasticity 25, 1879–1887.
Yang, J.L., Zhang, Z., Schlarb, A.K., Friedrich, K., 2006a. On the characterization of tensile creep resistance of polyamide 66 nanocomposites. Part I: Experimental results and general discussions. Polymer 47, 2791–2801.
Yang, J.L., Zhang, Z., Schlarb, A.K., Friedrich, K., 2006b. On the characterization of tensile creep resistance of polyamide 66 nanocomposites. Part II: Modeling and prediction of long-term performance. Polymer 47, 6745–6758.
Yang, J.L., Zhang, Z., Friedrich, K., Schlarb, A.K., 2007. Creep resistant polymer nanocomposites reinforced with multiwalled carbon nanotubes. Macromol. Rapid. Commun. 28, 955–961.
Zhang, W.X., Wang, T.J., Chen, X., et al, 2010. Effect of surface/interface stress on the plastic deformation of nanoporous materials and nanocomposites. Int. J. Plasticity 26, 957–975.